



**HAL**  
open science

## New particle formation from agricultural recycling of organic waste products

Raluca Ciuraru, Julien Kammer, Céline Décuq, Marin Vojkovic, Kawsar Haider, Yvain Carpentier, Florence Lafouge, C. Berger, Marjolaine Bourdat-Deschamps, Ismaël Ortega, et al.

► **To cite this version:**

Raluca Ciuraru, Julien Kammer, Céline Décuq, Marin Vojkovic, Kawsar Haider, et al.. New particle formation from agricultural recycling of organic waste products. *npj climate and atmospheric science*, 2021, 4 (1), pp.5. 10.1038/s41612-021-00160-3 . hal-03160367

**HAL Id: hal-03160367**

**<https://hal.science/hal-03160367v1>**

Submitted on 12 Jun 2024

**HAL** is a multi-disciplinary open access archive for the deposit and dissemination of scientific research documents, whether they are published or not. The documents may come from teaching and research institutions in France or abroad, or from public or private research centers.

L'archive ouverte pluridisciplinaire **HAL**, est destinée au dépôt et à la diffusion de documents scientifiques de niveau recherche, publiés ou non, émanant des établissements d'enseignement et de recherche français ou étrangers, des laboratoires publics ou privés.

# New particle formation from agricultural recycling of organic waste products

R Ciuraru<sup>1\*</sup>, J Kammer<sup>1</sup>, C Decuq<sup>1</sup>, M Vojkovic<sup>2</sup>, K Haider<sup>1,2</sup>, Y Carpentier<sup>2</sup>, F Lafouge<sup>1</sup>, C Berger<sup>1</sup>, M Bourdat-Deschamps<sup>1</sup>, I K. Ortega<sup>3</sup>, F Levavasseur<sup>1</sup>, S Houot<sup>1</sup>, B Loubet<sup>1</sup>, D Petitprez<sup>4</sup>, C Focsa<sup>2</sup>

<sup>1</sup>INRAE, Université Paris-Saclay, AgroParisTech, UMR ECOSYS, 78850, Thiverval-Grignon, France

<sup>2</sup>Univ. Lille, CNRS, UMR 8523, PhLAM – Laboratoire de Physique des Lasers Atomes et Molécules, F-59000 Lille, France

<sup>3</sup>Multi-physics for Energetics Department, ONERA Université Paris Saclay, F-91123, Palaiseau, France

<sup>4</sup>Univ. Lille, CNRS, UMR 8522, PC2A – Laboratoire de Physico-Chimie des Processus de Combustion de l'Atmosphère, F-59000 Lille, France

## Abstract

Secondary organic aerosols (SOA) are one of the main uncertainty sources in the current understanding of the Earth's Climate. It is known that agriculture contributes to primary aerosol emissions but there is no estimate for the secondary organic aerosol formation from precursor gas phase. Organic waste products like sewage sludge are applied to cropland as fertilizers. In this work we show that sewage sludge is an unaccounted source of nucleation precursors, as skatole (C<sub>9</sub>H<sub>9</sub>N). The skatole emission and nucleation rates up to 1.1x10<sup>6</sup> cm<sup>-3</sup> s<sup>-1</sup> due to ozone reactivity were measured in the laboratory. Our results show that SO<sub>2</sub> plays a key role in the oxidation of skatole and leads to intensive new particle formation. Products of the ozone reactions with skatole and the possible ozonolysis reaction mechanism are discussed. This novel nucleation mechanism might aid our understanding of the organic waste agricultural recycling contribution to the aerosol balance in the atmosphere. Based on the measured particle emission flux, the sewage sludge spread surface area in France and the time before sewage sludge incorporation into the soil, a rough estimation for the annual quantity of particles generated by this agricultural activity is on the range of one ton, which represents ~0.03% of the total PM<sub>1.0</sub> emissions from agriculture and forestry in France. As the spreading is concentrated on a few days (mid-summer), these emissions may punctually be of high concern for local and regional air quality during that period of the year.

## Introduction

Atmospheric aerosols constitute a major concern for human health and impact Earth's radiative balance both directly and indirectly, through their influence on cloud properties. Atmospheric aerosols act as cloud condensation nuclei, thus altering cloud albedo, structure, and lifetime. They also represent a major health and economic issue since the particulate pollution is responsible for approximately 3 million premature deaths per year and projected to increase to 6 million in 2050<sup>1</sup>. Volatile organic compounds (VOC), emitted into the atmosphere from anthropogenic and biogenic sources, are major players in atmospheric photochemical reactions that contribute to

34 ozone formation. VOCs are also responsible for secondary organic aerosol (SOA) formation in the presence of  
35 photo-oxidants <sup>2</sup>.

36 As stated by different model simulation and laboratory studies, the most important source of atmospheric aerosols,  
37 in terms of their number concentration and of climate-relevant particles, is new particle formation (NPF) and  
38 growth <sup>3</sup>. However, the nucleation mechanism leading to new particle formation remains not well understood.  
39 Sulfuric acid has been identified as a key compound in atmospheric new particle formation<sup>4</sup>, but its concentration  
40 in the atmosphere is too low to explain observed nucleation rates, so additional compounds are needed<sup>4</sup>. Base  
41 compounds such ammonia<sup>5</sup> or amines<sup>6</sup> have been proven to stabilize sulfuric acid clusters, leading to nucleation  
42 rates similar to those observed in the atmosphere. In addition, it has been shown that Highly Oxygenated Molecules  
43 (HOMs) coming from oxidation of VOCs, can as well stabilize sulfuric acid clusters<sup>7</sup>. Furthermore, a recent study<sup>8</sup>  
44 found that HOMs are able to form particles without the participation of sulfuric acid.

45 Measurements have quantified the formation of these compounds from ozonolysis of monoterpenes <sup>9</sup> and  
46 modelling studies have quantified their formation in the atmosphere and their role in air quality <sup>10,11</sup>. However, our  
47 understanding of the processes of formation and aging of organic aerosols remains very limited but entirely  
48 necessary to improve the robustness of the models <sup>12</sup>.

49 It is now well known that agriculture and its activities affect local, regional and global air quality and global climate  
50 by its significant ammonia (NH<sub>3</sub>) and greenhouse gases (GHG) emissions but also through VOC and aerosol  
51 emissions <sup>13</sup>. In some regions (e.g. eastern USA, Europe, Russia and East Asia) agricultural emissions are estimated  
52 to be the largest relative contribution to PM<sub>2.5</sub> <sup>14</sup>. Agriculture represents also a major ground-level ozone sink <sup>15</sup>.  
53 A wide variety of pollutants and GHGs, especially nitrogen containing compounds, are emitted to the atmosphere  
54 from agricultural activities, including fertilizers use, farm machinery or livestock manure spreading. In particular,  
55 in France, agriculture is estimated to generate about one third of the annual particle emissions (e.g. from livestock  
56 housing and tilling activities), a number still highly uncertain <sup>16</sup>. While great efforts have been made to estimate  
57 GHG and NH<sub>3</sub> emissions from agriculture and explore ways to abate them, knowledge about other pollutants  
58 emitted by this sector is still scarce, in particular on SOA and VOC precursors. Agricultural activities involving  
59 fertilizers or pesticides are also known to emit VOCs with high SOA forming potential <sup>14</sup>. However, the current  
60 knowledge mainly accounts for the effect of ammonia on PM formation. A recent study <sup>17</sup> testing reduction  
61 scenarios of agricultural emissions showed that in many densely populated areas, PM<sub>2.5</sub> aerosols formed from  
62 gases released by fertilizer application and animal husbandry can dominate over the combined contributions from  
63 all other anthropogenic pollution. The authors showed that the impact of livestock and fertilizers on air quality is

64 very pronounced in Europe, where agricultural PM<sub>2.5</sub> is responsible for 55% of air pollution linked to human  
65 activities <sup>17</sup>.

66 The recycling of different types of organic waste products (OWP) from livestock, urban or industrial sources is  
67 currently being promoted as a substitute for mineral fertilizers for agricultural land <sup>18</sup>. The recycling of OWP  
68 represents also an alternative to waste management by landfilling or incineration. The OWP recycling in  
69 agriculture can increase the organic matter stocks in soil <sup>19</sup> and thereby improve soil chemical fertility, stimulate  
70 microbial activity or increase water retention <sup>20</sup>. It also improves the recycling of nutrients and can decrease the  
71 use of mineral fertilizers <sup>21</sup> which are non-renewable resources. However, the application of OWP to agricultural  
72 soils can present different health and environmental risks: some contaminants can accumulate in the soil, degrade  
73 water quality or be emitted into the atmosphere <sup>22</sup>. In a peri-urban context, where the number of municipal  
74 wastewater treatment plants is continuously increasing through urbanization, the sewage sludge production  
75 increased by 50% in European countries from 1992 to 2005 and a further increase of the total sludge production  
76 is being expected in the upcoming years <sup>23</sup>. Concerning the sludge final disposal, it has been shown that 53% of  
77 the production is used in agricultural application and composting <sup>24</sup>.

78 In spite of the continuously increasing number of atmospheric new particle formation measurements, we are still  
79 lacking regional observations of NPF processes. This is the case for agricultural areas where we have only limited  
80 understanding of the biosphere-atmosphere exchange of agriculturally emitted trace gases other than NH<sub>3</sub>, whilst  
81 their contribution to secondary aerosol is missing <sup>13</sup>. The importance of agriculture on atmospheric NPF is expected  
82 to vary regionally, as well as over the course of the year.

83 Some studies already showed VOC emissions from organic fertilizers by laboratory measurements or small wind  
84 tunnel experiments <sup>25,26,27</sup>. To our knowledge, no work addressed to date their contribution to SOA. For instance,  
85 there are few studies dealing with VOC measurements from livestock fertilizers <sup>27,28</sup> or urban waste products <sup>29,30</sup>,  
86 although such data are essential for a better understanding of the formation and fate of SOA from agricultural  
87 practice. Research on VOC emissions was demonstrated to be very challenging due to the large number of VOCs  
88 and their variation in physicochemical properties <sup>31</sup>. Our understanding of the chemistry of these VOCs is very  
89 limited compared to other agricultural pollutants, like NH<sub>3</sub> or, more recently, hydrogen sulfide <sup>32,33</sup>. However, a  
90 certain number of VOCs observed in organic waste are now established precursors for SOA, such as: sulfur  
91 compounds (e.g. dimethyl and diethyl sulfide) <sup>28,34</sup>, terpenes (alpha-pinene, limonene) <sup>30</sup>, nitrogen containing  
92 compounds, ketones and aldehydes <sup>35</sup>, aromatic compounds <sup>29,31,36</sup>.

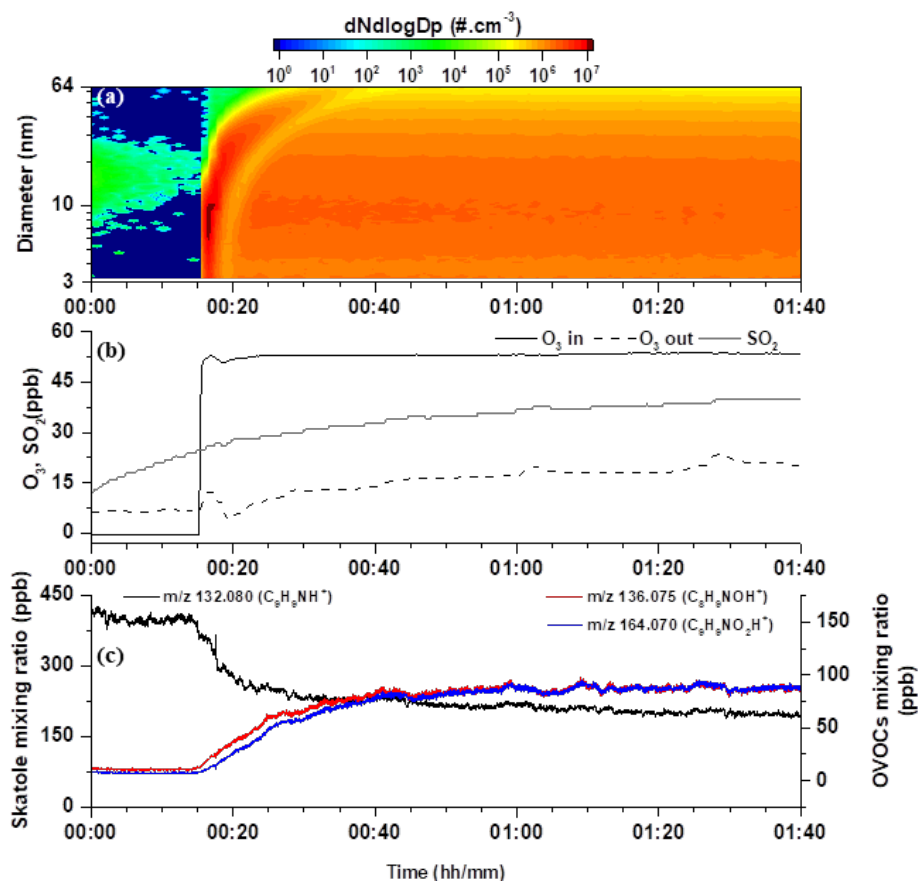
93 Simulations and atmospheric observations show that almost all nucleation processes involve ammonia or biogenic  
94 organic compounds in addition to sulfuric acid<sup>3</sup>. Up to now, the agricultural secondary aerosol formation is thought  
95 to be mainly induced by nucleation of ammonia emissions<sup>14</sup>. Here we report atmospheric particle formation solely  
96 from oxidized organic molecules and SO<sub>2</sub>, both emitted by sewage sludge. The focus of this work is to identify  
97 the molecules that form new particles from sewage sludge and to understand the mechanism underlying particle  
98 formation and their initial growth. To the best of our knowledge, this is the first time these aerosol formation  
99 phenomena have been observed and quantified in an agricultural system.

## 100 **Results**

### 101 **Evidence of new particle formation from sewage sludge**

102 Sewage sludge samples from a sewage treatment plant were introduced into a Teflon coated reaction chamber and  
103 exposed to ambient levels of ozone (Supplementary Figure S1). Prior to each ozonolysis experiment, the chamber  
104 was carefully cleaned, and extremely low contaminant concentrations were established (Supplementary FigureS2).  
105 Upon the sample introduction into the chamber, a strong burst release of methylindole ( $m/z$  132.087 C<sub>9</sub>H<sub>9</sub>NH<sup>+</sup>)  
106 was observed. Following the initial burst, sewage VOC signals stabilized. A production of NH<sub>3</sub> and SO<sub>2</sub> was also  
107 observed. NO<sub>x</sub> mixing ratios were low (2-3 ppb) during the experiments. Within a few seconds of the initial  
108 exposure of sewage sludge samples to O<sub>3</sub> in the chamber, the signal of  $m/z$  132.087 C<sub>9</sub>H<sub>9</sub>NH<sup>+</sup> decreased and gas-  
109 phase oxygenated and nitrogen containing molecules increased, in particular  $m/z$  136.075 C<sub>8</sub>H<sub>9</sub>NOH<sup>+</sup> and  $m/z$   
110 164.070 C<sub>9</sub>H<sub>9</sub>NO<sub>2</sub>H<sup>+</sup> (Figure 1c). The ozone mixing ratio was continuously monitored into the chamber and  
111 remained at around 55 ppbv at the entrance of the chamber during each experiment. Particles appeared almost  
112 instantaneously after O<sub>3</sub> injection. The particle number and size distributions (Figure 1a) span the entire measured  
113 size range from 2 to 64 nm electrical mobility diameters, therefore showcasing newly formed particles. During  
114 these experiments, the particle number concentration reached a maximum of 10<sup>6</sup> particles cm<sup>-3</sup> within less than 2  
115 min. This lead to a particle nucleation rate up to 1.1x10<sup>6</sup> cm<sup>-3</sup> s<sup>-1</sup> during the new particle formation process. At  
116 longer reaction times, the particles grew in size and their number remained constant thereafter or slightly decreased  
117 probably due to coagulation and/or losses by adsorption to the walls. This behavior of particle number  
118 concentration and size distribution was observed to be constant for experiments as long as five hours.  
119 Interestingly, the ozone was not completely consumed during the experiment, which means that only around 20  
120 ppb of O<sub>3</sub> were needed for the ozonolysis to form particles. Additional experiments performed in high excess of  
121 ozone (250 ppb) did not show any difference in particle number and size distribution. This may indicate that the  
122 reaction is limited by the residence time (5 min) inside the chamber. A fast but not complete consumption of  $m/z$

123 132.087  $C_9H_9NH^+$  was also observed and the reaction products reached a plateau in less than 15 min. This may be  
 124 due to the high kinetic rate constant of  $m/z$  132.087  $C_9H_9NH^+$  reaction with ozone but might also indicate that the  
 125 oxidation can occur in both gas and condensed phases (walls, sewage sludge surface or secondary aerosols).



126  
 127 Figure 1. Typical sewage sludge ozonolysis experiment. (a) Temporal evolution of particle number concentration  
 128 and size distribution. The ordinate represents the electrical mobility diameter (nm) and the color scale the particle  
 129 number concentration. (b) Temporal evolution of  $O_3$  entering the chamber (black line,  $O_3$  in),  $O_3$  measured at the  
 130 exit of the chamber (black dotted line,  $O_3$  out) and  $SO_2$  (grey line). (c) Temporal evolution of  $m/z$  132.080  
 131  $C_9H_9NH^+$  (black line, left axis),  $m/z$  136.075  $C_8H_9NOH^+$  (red line, right axis) and  $m/z$  164.070  $C_9H_9NO_2H^+$  (blue  
 132 line, right axis).

### 133 Identification of key players in new particle formation

134 A comparison of the VOC data measured with three independent techniques (proton-transfer reaction mass  
 135 spectrometry - PTR-ToF-MS; gas chromatography coupled to mass spectrometry - GC-MS and ultra-high  
 136 performance liquid chromatography coupled to high-resolution mass spectrometry - UHPLC-HRMS) was  
 137 performed to identify the detected ions. The identification was based on each compound retention time and mass  
 138 spectrum. The  $m/z$  132.08  $C_9H_9NH^+$  was identified as skatole. Skatole has been showcased as one of the major  
 139 malodorous compounds contributing to the odor problem of animal production facilities and sewage treatment

140 plants being emitted by bacterial degradation in slurry<sup>32,37</sup>. Indoles belong to an important class of atmospheric  
141 VOCs with high emissions from land spreading of organic waste products to the atmosphere and contribute to odor  
142 nuisance<sup>27,38</sup>.

143 It was reported that indoles and skatole are very reactive nucleophiles and easily undergo electrophilic substitution  
144 reactions<sup>39</sup>. Only one study reported the reaction rate constant in aqueous phase for skatole with ozone at pH=6.7  
145 as being  $4.5 \times 10^6 \text{ M}^{-1} \text{ s}^{-1}$ <sup>40</sup>. The authors reported a stoichiometric factor of 0.9 meaning that 1 mol of ozone is  
146 needed for ozonation of 0.9 mol of skatole<sup>40</sup>, the reaction rate constants of the indolic compounds in water increase  
147 with pH. A rough estimation of the rate constant, using skatole experiments, has been performed. We estimated  
148 the rate constant of  $5 \times 10^{-15} \text{ cm}^3 \text{ mol}^{-1} \text{ s}^{-1}$ . Such a rate constant would confirm that skatole is a very reactive  
149 compound towards ozone, leading to a lifetime of around 3 minutes at typical ozone ambient concentrations. This  
150 is a higher reactivity than what was reported for indole ( $5 \times 10^{-17} \text{ cm}^3 \text{ mol}^{-1} \text{ s}^{-1}$ )<sup>41</sup>, or the well-known alpha-pinene  
151 system ( $1 \times 10^{-16} \text{ cm}^3 \text{ mol}^{-1} \text{ s}^{-1}$ )<sup>42</sup>, but lower than a few alkenes such as the alpha-terpinene or beta-caryophyllene.

152 As shown in Figure 1 c, two oxygenated products were observed in the gas phase ( $m/z$  136.075  $\text{C}_8\text{H}_9\text{NOH}^+$  and  
153  $m/z$  164.070  $\text{C}_9\text{H}_9\text{NO}_2\text{H}^+$ ) subsequent to ozonolysis reactions. These oxidation products contain the carbon  
154 skeleton of their precursor skatole. Gas chromatography analysis performed before and after ozonolysis and liquid  
155 chromatography performed on collected particles revealed that  $m/z$  164.070  $\text{C}_9\text{H}_9\text{NO}_2\text{H}^+$  corresponds to 2-acetyl  
156 phenyl formamide.

157 Multiple other VOCs were emitted by the sewage sludge samples. For example, acids (e.g. formic acid), alcohols  
158 (e.g. methanol, butanol), aldehydes and ketones (acetone, butanone, acrolein) or sulfur containing compounds (e.g.  
159 dimethyl sulfide, hydrogen sulfide) were measured but most of these VOCs react very slowly with ozone. Isoprene  
160 and monoterpenes have been also measured by PTR-TOF-MS in our experiments. However, all the ion signals  
161 were carefully verified and the only decreasing ion that was observed, based on the PTR-TOF-MS measurements,  
162 was the one of skatole. We cannot fully exclude that other VOCs might play a role in the particle formation but,  
163 from our experiments, skatole is the only VOC that has been evidenced as aerosol precursor.

### 164 **Proposed ozonolysis mechanism**

165 The reaction of ozone with skatole proceeds by the Criegee mechanism by an initial  $\text{O}_3$  addition to the double  
166 bond to yield a primary ozonide which decomposes into two stabilized Criegee intermediates (Figure 2)<sup>43</sup>. Since  
167 the ozonolysis of skatole is taking place at the endocyclic double bond, the carbonyl oxide and carbonyl moieties  
168 that should be formed are attached together as part of the same molecule<sup>44,45</sup>. The ozonolysis of endocyclic

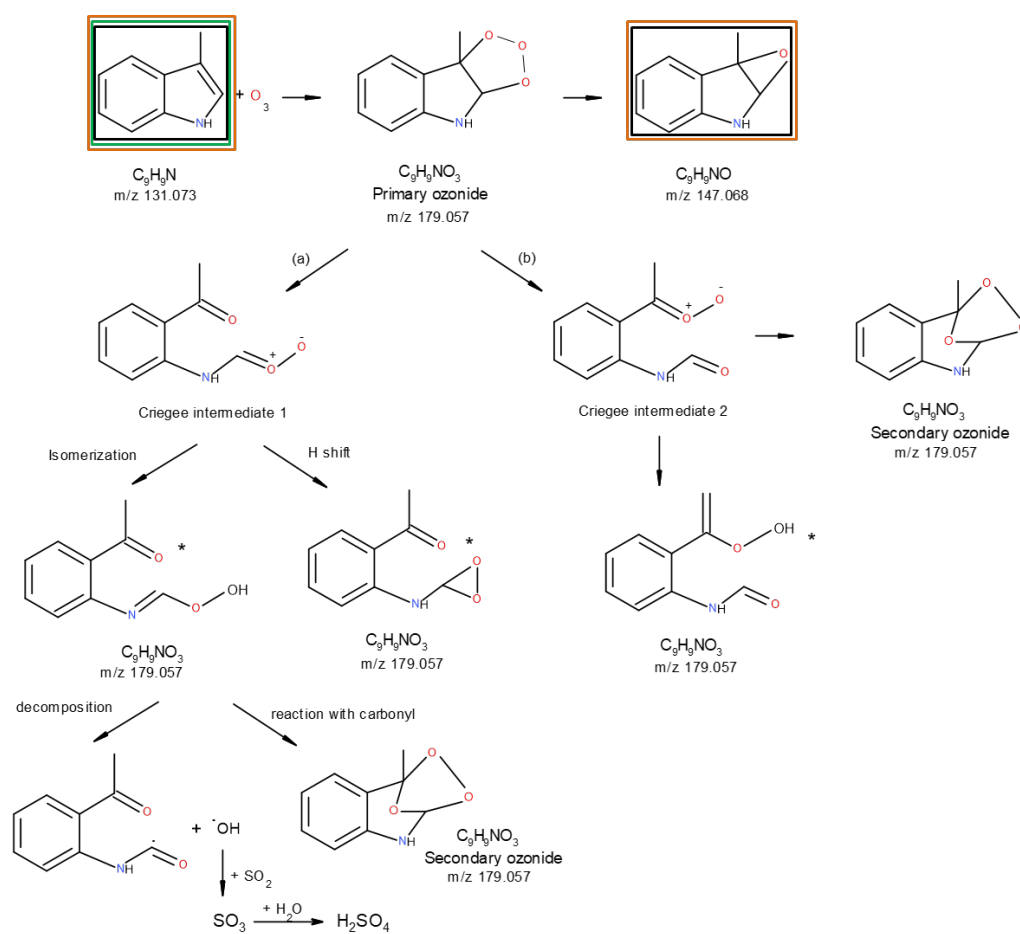
169 compounds may add several functional groups with no loss in carbon number leading further to the formation of  
170 secondary ozonides which has been shown to have an important contribution to SOA <sup>2</sup>.

171 The primary ozonide has two possible channels: decomposition by cycle cleavage of the O-O bond distal from the  
172 methyl group (a) or cleavage of the O-O bond proximal to the methyl (b). The first intermediate can undergo  
173 hydrogen shift reactions to form ketonic hydroperoxides or can isomerize to form a dioxirane<sup>43</sup>. The second  
174 intermediate leads to aldehydic hydroperoxides or cyclizes to form a secondary ozonide. Both can form a  
175 secondary ozonide via recyclization <sup>43,45</sup> (Figure 2). The further decomposition of of the O-OH bond in the  
176 hydroperoxides, which are thermally unstable<sup>47</sup>, will lead to organic and OH radicals formation <sup>48</sup>. On the other  
177 hand, the Criegee intermediate 1 can react with a carbonyl and form the secondary ozonide C<sub>9</sub>H<sub>9</sub>NO<sub>3</sub> (m/z  
178 179.057)<sup>43</sup>. The first intermediate can oxidize SO<sub>2</sub> and form the 2-acetyl phenyl formamide C<sub>9</sub>H<sub>9</sub>NO<sub>2</sub> (m/z  
179 163.063) and SO<sub>3</sub>. Hydrolysis of SO<sub>3</sub> leads to the further formation of H<sub>2</sub>SO<sub>4</sub>. It has been shown that reactions of  
180 Criegee intermediates formed in ozonolysis of certain alkenes with SO<sub>2</sub> can be significantly fast <sup>49</sup>. It has also been  
181 shown that this reaction is characterized by 97% collisional stabilization and only a few percent of ring opening  
182 and SO<sub>3</sub> formation<sup>50</sup>. The secondary ozonide (C<sub>9</sub>H<sub>9</sub>NO<sub>3</sub>) can react with water to form a molecule possessing an  
183 aldehyde or a ketone group and a hydroxy-hydroperoxide group (Figure 2). The latter compound can lose H<sub>2</sub>O<sub>2</sub>  
184 and form the 2-acetyl phenyl formamide. Further oxidation of this compound leads to an oxocarboxylic acid  
185 evidenced on the aerosol surface by two-step laser mass spectrometry (L2MS). Another possibility is that the  
186 hydroxy-hydroperoxide group loses water and thus 2-acetyl phenyl formamide is directly formed. Skatole oxide  
187 was also observed in the gas phase due to the ozonolysis reaction (m/z 148.075 C<sub>9</sub>H<sub>9</sub>NOH<sup>+</sup>). It is now known that  
188 oxidation of SO<sub>2</sub> by stabilized Criegee intermediates represents a significant source for atmospheric sulfuric acid  
189 production via SO<sub>3</sub> formation. The SO<sub>3</sub> reacts very rapidly with water vapor to form H<sub>2</sub>SO<sub>4</sub> <sup>49</sup> which is a key  
190 atmospheric nucleation species <sup>45</sup>. The production of OH radicals during the ozonolysis of the indole will drive  
191 further chemistry, including oxidation of SO<sub>2</sub> to H<sub>2</sub>SO<sub>4</sub> <sup>49</sup>. Various field measurements and modeling studies  
192 showed that stabilized Criegee intermediates could make a significant contribution (from 10 to 70%) to SO<sub>2</sub>  
193 oxidation <sup>44</sup>. It has been shown that oxidation of SO<sub>2</sub> by stabilized Criegee intermediate is a significant source for  
194 atmospheric sulfuric acid production in VOC-rich environments <sup>45</sup>. The SO<sub>2</sub> emitted by the sewage sludge samples  
195 will react then with Criegee intermediates to produce sulfuric acid. Moreover, SO<sub>2</sub> can also partition into aerosol  
196 to form HSO<sub>3</sub><sup>-</sup> that can further react with organic peroxides generated by skatole ozonolysis. This mechanism is  
197 consistent with literature data <sup>51</sup> and with the presence of this type of species on our collected particles. Secondary  
198 ion mass spectrometry (SIMS) surface analysis performed (in negative ion polarity) on the newly formed particles

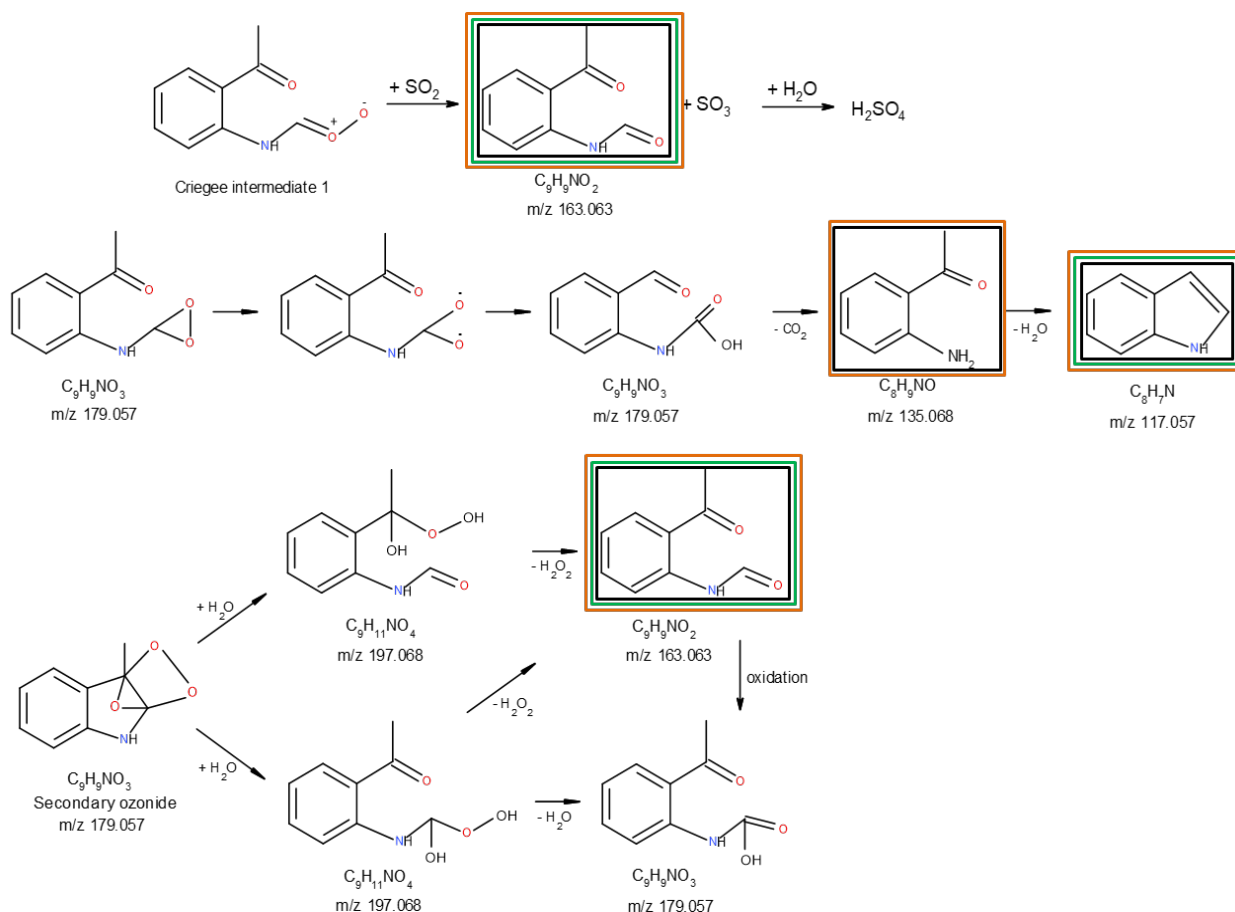


199 collected on quartz filters during ozonolysis reactions revealed the presence of the characteristic  $\text{H}_2\text{SO}_4$  peaks such  
 200 as  $\text{SO}_3^-$  and  $\text{HSO}_4^-$  (Supplementary Fig. S4). We note that  $\text{SO}_3^-$  and  $\text{HSO}_4^-$  ions were also detected in the sewage  
 201 sludge bulk samples by SIMS (Supplementary Fig. S5). No sulfur containing organic compounds were detected  
 202 in the present study, but it cannot be excluded that organosulfates may have fragmented in the SIMS, contributing  
 203 to the observed  $\text{SO}_3^-$  signal.

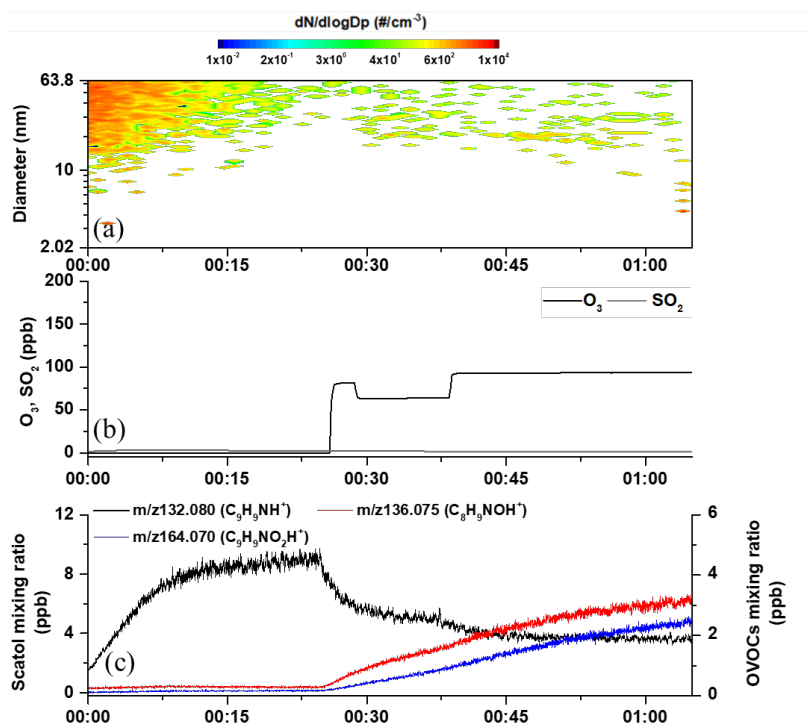
204 Another important channel is the reaction of stabilized Criegee intermediates with water, leading to the formation  
 205 of  $\alpha$ -hydroxy hydroperoxides, organic acids, ketones and aldehydes,  $\text{SO}_2$ ,  $\text{NO}_x$ ,  $\text{H}_2\text{O}_2$  <sup>44</sup>. These reactions may also  
 206 represent a significant source of OH and HOx radicals <sup>43</sup>. The observed products can therefore arise from the  
 207 reaction of both ozone and OH radicals with these compounds.



208



225 Furthermore, some other experiments performed on non-SO<sub>2</sub> emitting sewage samples showed no particle  
 226 formation following skatole ozonolysis (Figure 3). In light of these results, we are advancing a binary reaction  
 227 mechanism of organics and SO<sub>2</sub> via sulfuric acid formation.



228  
 229 Figure 3. Non emitting SO<sub>2</sub> sewage sludge ozonolysis experiment . (a) Temporal evolution of particle  
 230 concentration and size distribution. The ordinate represents the electrical mobility diameter (nm) and the color  
 231 scale the particle number concentration. (b) Temporal evolution of O<sub>3</sub> entering the chamber (black line, O<sub>3</sub> in), and  
 232 SO<sub>2</sub> (grey line). (c) Temporal evolution of m/z 132.080 C<sub>9</sub>H<sub>9</sub>NH<sup>+</sup> (black line, left axis), m/z 136.075 C<sub>8</sub>H<sub>9</sub>NOH<sup>+</sup>  
 233 (red line, right axis) and m/z 164.070 C<sub>9</sub>H<sub>9</sub>NO<sub>2</sub>H<sup>+</sup> (blue line, right axis).

234 Several studies performed on sewage sludge samples or sewage sludge compost showed the presence of different  
 235 inorganic and sulfur organic compounds (hydrogen sulfide, methyl mercaptan, dimethyl sulfide, dimethyl  
 236 disulfide, carbon disulfide) produced by anaerobic microorganisms. Sulfur-containing compounds are also  
 237 produced by bacteria through the reduction of sulfate and S-containing amino acids<sup>52,53</sup>. Amino acids are the  
 238 monomers of protein that have been shown to be present in protein extracted from activated sludges and  
 239 anaerobically digested sludges. Organic sulfur compounds from dewatered biosolids can be generated by the  
 240 degradation of sulfur-containing amino acids and methylation of sulfide and methanethiol. Furthermore, the  
 241 thermal utilization of sewage sludge leads to the emission of pollutants in the form of sulfur dioxide<sup>53</sup> and it has  
 242 also been shown that sewage sludge can contain high concentrations of sulphur compounds and emissions of  
 243 sulphur dioxide (SO<sub>2</sub>)<sup>34</sup>. H<sub>2</sub>S reacts rapidly with OH radicals with a rate constant of  $4.7 \times 10^{-12}$  cm<sup>3</sup> molecule<sup>-1</sup> s<sup>-1</sup>

244 and form SO<sub>2</sub>. It is possible then that the SO<sub>2</sub> is formed by these reactions in our system. On the other hand, the  
245 reaction of H<sub>2</sub>S with ozone is too slow to form SO<sub>2</sub> in our experiments<sup>54</sup>.

#### 246 **Testing the skatole new particle formation hypothesis**

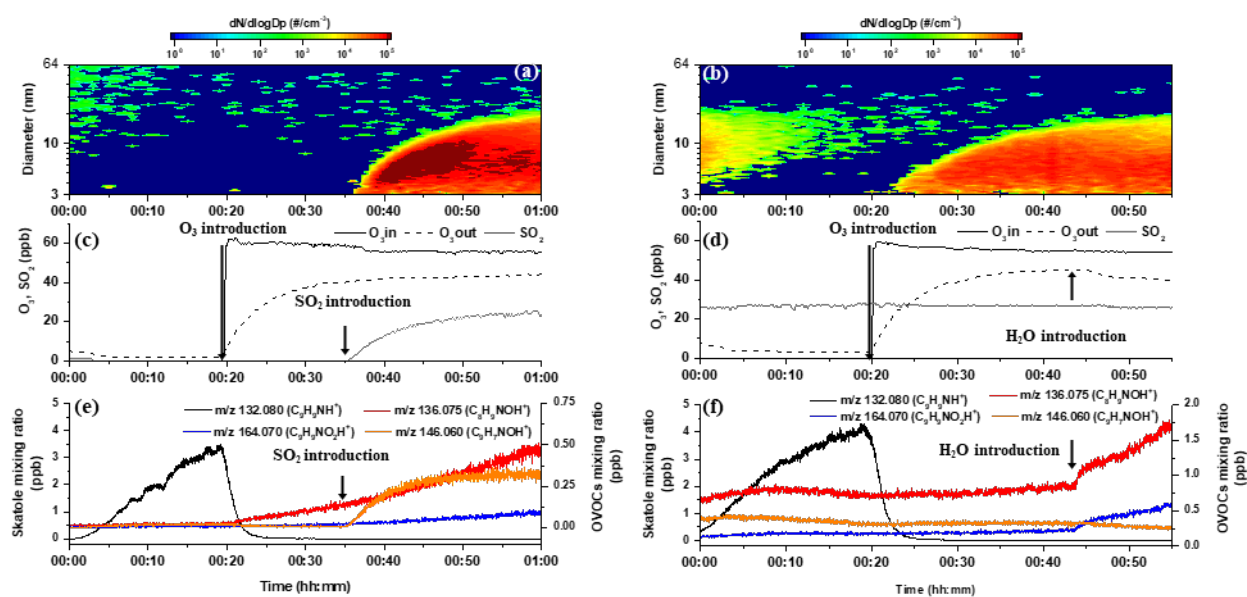
247 To verify this hypothesis, we designed an experiment in which skatole reactivity was measured in the empty  
248 chamber. The goal was to test the effect of O<sub>3</sub>, SO<sub>2</sub> and NH<sub>3</sub> on commercially available skatole. A pure skatole  
249 sample was introduced into the chamber and, as shown in Figure 4, the skatole signal drops dramatically after the  
250 O<sub>3</sub> introduction and is accompanied by a slow increase of m/z 136.075 C<sub>8</sub>H<sub>9</sub>NOH<sup>+</sup> and m/z 164.07 C<sub>9</sub>H<sub>9</sub>NO<sub>2</sub>H<sup>+</sup>.  
251 The reaction of ozone with skatole proceeds by initial O<sub>3</sub> addition to the double bond to yield a primary ozonide.  
252 However, no particle formation was observed following ozonolysis therefore, we can discard the pure biogenic  
253 nucleation mechanism. Most likely the volatility of skatole oxidation products is not low enough. Upon SO<sub>2</sub>  
254 introduction into the chamber, the formation of m/z 146.060 C<sub>9</sub>H<sub>7</sub>NOH<sup>+</sup> was observed, which may represent the  
255 product of the hydroperoxide channel of the Criegee intermediate (Figure 2). The m/z 136.060 C<sub>8</sub>H<sub>7</sub>NOH<sup>+</sup>,  
256 corresponding to the ester channel of the Criegee intermediate, was also observed in the gas phase after SO<sub>2</sub>  
257 introduction. The contribution of SO<sub>2</sub> in new particle formation is further illustrated in Figure 4, which shows the  
258 prompt NPF event only once the SO<sub>2</sub> is introduced into the chamber. This is consistent with sulfuric acid formation  
259 by reactions of sulfur dioxide with stabilized Criegee intermediates<sup>45</sup>. Most likely oxidation products of skatole  
260 are able to stabilize sulfuric acid clusters enhancing NPF event observed. Skatole itself is a base compound, with  
261 a similar proton affinity to the one for dimethyl amine (DMA), which has been found to be a key player in  
262 atmospheric nucleation<sup>6</sup>. From a molecular point of view, the key for stabilization of molecular clusters of bases  
263 with sulfuric acid is the proton transfer<sup>55</sup>, as in the case of, e.g., ammonia and sulfuric acid clusters. Classical  
264 nucleation theory (CNT) use bulk properties, so it predicts a proton transfer from the very first cluster containing  
265 one sulfuric acid molecule and one ammonia molecule. However, quantum mechanics (QM) chemical calculations  
266 have shown that this is not the case, as one will need at least two molecules for the proton to be transferred. When  
267 translating it in terms of evaporation rates of cluster calculated by CNT and QM, this leads to differences of several  
268 orders of magnitude. In the case of DMA, the proton transfer happens from the very beginning, with just one  
269 molecule of sulfuric acid; this explains why DMA can enhance nucleation of sulfuric acid much more than  
270 ammonia<sup>8,55</sup>. This is the reason why we compare DMA to skatole in terms of proton affinity. In addition, other  
271 important molecular feature for a base to be able to enhance nucleation effectively seems to be having an additional  
272 H atom attached to the N atom so it can form hydrogen bonds with more than one sulfuric acid molecule<sup>55</sup>. Skatole,  
273 as DMA, presents a hydrogen atom attached to the N atom, so we think that this might as well be an advantage for

274 skatole enhancing sulfuric acid nucleation as in the case of DMA. Dedicated quantum chemical calculations, out  
275 of the scope of this paper, might be interesting in this case and could confirm our hypothesis.

276 Other base compounds as indole are produced during skatole oxidation. Furthermore, all oxidation products of  
277 skatole keep the N atom in their structure, even if they might have as well a carboxylic acid group. From a  
278 molecular point of view, having both a NH group and a carboxylic acid group can facilitate the formation of  
279 clusters with several molecules of sulfuric acid. Indeed, the theoretical simulations done by Elm et al.<sup>56</sup> shows how  
280 small amino-acids can effectively stabilize sulfuric acids clusters, thus playing an important role in atmospheric  
281 NPF. Aerosol number concentration reaches its maximum when SO<sub>2</sub> is introduced. It is also interesting to observe  
282 the different particle size: smaller particles are formed in skatole controlled experiments compared to sewage  
283 sludge experiments, revealing the potential role of other VOCs that might contribute to particles growth. In a  
284 second step, ozone was introduced into the chamber while skatole and SO<sub>2</sub> mixing ratios were kept constant.  
285 Likewise, the skatole signal decreased shortly after O<sub>3</sub> was added (Figure 4f), accompanied by a concurrent new  
286 particle formation event (Figure 4b), confirming the need of sulfuric acid and oxidation products of skatole to  
287 produce new particles.

288 In a third step, water vapor was added into the chamber (from dry conditions to 90% RH). As shown in Figure 4f,  
289 the water introduction led to an increase of the m/z 136.075 C<sub>8</sub>H<sub>9</sub>NOH<sup>+</sup> and m/z 164.07 C<sub>9</sub>H<sub>9</sub>NO<sub>2</sub>H<sup>+</sup> signals in the  
290 gas phase. The stabilized Criegee m/z 146.060 C<sub>9</sub>H<sub>7</sub>NOH<sup>+</sup> is slightly decreasing. It might then react with water  
291 vapor to form a carbonyl compound and H<sub>2</sub>O<sub>2</sub>. The increase of m/z 164.070 in presence of water indicates a  
292 possible competition between the water vapor and the Criegee intermediates. In the first set of experiments when  
293 RH is very low (Figure 4e), one can observe the formation of m/z 146.060 C<sub>9</sub>H<sub>7</sub>NOH<sup>+</sup> when introducing SO<sub>2</sub>,  
294 while at high RH the formation of 2-acetyl phenyl formamide is detected. In contrast, water vapor showed no  
295 effect on the aerosol particle number concentration.

296 The same types of experiments were performed to test the NH<sub>3</sub> effect on the new particle formation. As in the case  
297 of SO<sub>2</sub>, the NH<sub>3</sub> was injected into the chamber during skatole ozonolysis. No new particle formation was observed  
298 when injecting NH<sub>3</sub> (Figure S3). Seeing these results, we can conclude that most likely the NPF mechanism behind  
299 the observed nucleation evens consist in sulfuric acid nucleation enhanced by the oxidation products of skatole  
300 acting as a base, like in the case of ammonia or amine nucleation reported in literature<sup>5,6</sup>.



301  
 302 Figure 4. Skatole ozonolysis experiment. (a, b) Temporal evolution of particle number concentration and size  
 303 distribution; (c, d) Temporal evolution of O<sub>3</sub> entering the chamber (black line), O<sub>3</sub> measured at the exit of the  
 304 chamber (black dotted line) and SO<sub>2</sub> (grey line); (e, f) Temporal evolution of m/z 132.080 C<sub>9</sub>H<sub>9</sub>NH<sup>+</sup> (black line,  
 305 left axis), m/z 136.075 C<sub>8</sub>H<sub>9</sub>NOH<sup>+</sup> (red line, right axis), m/z 146.060 C<sub>9</sub>H<sub>7</sub>NOH<sup>+</sup> (orange line, right axis) and m/z  
 306 164.070 C<sub>9</sub>H<sub>9</sub>NO<sub>2</sub>H<sup>+</sup> (blue line, right axis). Left column: SO<sub>2</sub> introduction at 00:35 min; right column: H<sub>2</sub>O  
 307 introduction at 00:43 min.

### 308 Atmospheric implications

309 This study gives new insights into the gaseous emissions and aerosol formation from organic waste products. It  
 310 clearly points toward an impact of the processes at the air - soil interface.

311 It has been shown that the agriculture contributes to about 16% of the PM<sub>2.5</sub> primary emissions and to ~18% of the  
 312 PM<sub>10</sub> emissions<sup>13</sup>. However, there is no estimate for the secondary organic aerosol formation from precursor gases  
 313 emitted by agriculture<sup>14</sup>. Recent studies show that aerosol formation in regions of intensive ammonia emission  
 314 may have been underestimated. A large part of the gap between modeled and measured aerosol concentrations  
 315 might be explained by these underestimated agricultural sources<sup>14</sup>. Moreover, agricultural particles were thought  
 316 to be generated during the specific operations and processes or secondary formed due to NH<sub>3</sub> emissions. In this  
 317 study, a new particle formation mechanism from agriculture that does not involve ammonia is highlighted.

318 This study shows that indoles, and more specifically skatole, together with SO<sub>2</sub> emitted by sewage sludge, are the  
 319 species pertinent to initiate reactions with atmospheric relevant ozone mixing ratios leading to particle nucleation  
 320 and growth events. The indole compounds are present at field scale during spreading on agricultural surfaces. For  
 321 example, skatole production and release of 4.91 - 8.3 μg m<sup>-2</sup> min<sup>-1</sup> following land spreading of pig slurry<sup>27</sup> or land  
 322 application of swine manure slurry<sup>57</sup> have been shown in the literature. Our emissions are estimated at around 50

323  $\mu\text{g m}^{-2} \text{min}^{-1}$  of skatole (details in Supplementary Information). Various reaction products were observed in the  
324 gas and particulate phases. Among them, 2-acetylphenyl formamide was identified as the main skatole ozonolysis  
325 product and formation pathways were proposed. Furthermore, the chemical analysis of particles shows that organic  
326 compounds contribute to growth in this size range. All these statements are supported by chamber measurements  
327 using commercially available skatole. The high reactivity of skatole towards ozone results in considerable  
328 enhancement of condensable reaction products that might partition into the aerosol phase and potentially act as  
329 cloud condensation nuclei<sup>3</sup>.

330 The particle mass ( $2.9 \mu\text{g m}^{-3}$ ) and number ( $5 \times 10^6 \# \text{cm}^{-3}$ ) concentrations measured in our experiments exceed  
331 some of field measurements conducted at various locations or other laboratory experiments performed on  
332 agricultural samples. Our study shows a particle nucleation rate up to  $1.1 \cdot 10^6 \text{ cm}^{-3} \text{ s}^{-1}$  during the new particle  
333 formation process. For example, the laboratory study of Joutsensaari *et al*<sup>58</sup> found aerosol number concentration  
334 of  $5.5 \times 10^3 \# \text{cm}^{-3}$  from the ozonolysis of volatile organic compounds emitted by white cabbage living plants and  
335 a particle formation rate of around  $3 \text{ cm}^{-3} \text{ s}^{-1}$  (over the particle diameter range 5.5 - 70 nm). Our numbers are higher  
336 than the particle formation rates observed in the atmosphere, which are often in the range of  $0.01\text{-}10 \text{ cm}^{-3} \text{ s}^{-1}$  in the  
337 boundary layer (for 3 nm particle). However, it has been shown that in urban, coastal areas or industrial plumes  
338 the formation rates are higher, up to  $100 \text{ cm}^{-3} \text{ s}^{-1}$  and  $10^4\text{-}10^5 \text{ cm}^{-3} \text{ s}^{-1}$  respectively<sup>12</sup>. In our experiments,  
339 emissions are constrained by the volume of the chamber. In the real atmosphere, they would be certainly more  
340 diluted, leading to a lower concentration of precursors. However, in the chamber, the reaction time is limited to  
341 the residence time (5 minutes). In the atmosphere, the ozonolysis of skatole will not be limited to 5 minutes, thus  
342 oxidation will occur all along the emission plume. It is obvious that longer oxidation will conduct to more oxidized  
343 compounds that will contribute to particle formation. Finally, even if our results are difficult to compare with real  
344 atmospheric processes, they evidenced the huge potential of sludge emissions as a strong contributor to particle  
345 formation.

346 Based on the particle emission flux in our experiments, on the sewage sludge spread surface area in France and on  
347 the time before sewage sludge incorporation into the soil (48 h, according to the French legislation), our results  
348 would yield a contribution of 0.94 tons particles per year. This value represents 0.03 % of  $\text{PM}_{1.0}$  total emissions  
349 from agriculture and forestry in France based on annual national emissions inventories (details in Supplementary  
350 Information). Given that spreading of sewage sludge takes place only on a few days per year, usually in the middle  
351 of the summer, the punctual contribution at this time of the year will not be negligible compared to other PM  
352 emission sources. The emissions from agriculture may be of concern for local and regional of air quality during

353 the time after spreading. These numbers would be higher if particle number instead of particle mass is considered.  
354 Indeed, high nucleation rates were observed, but the newly formed particles have a very low diameter and, as a  
355 result, a low mass. New particle formation from organic waste product spreading contributes significantly to  
356 atmospheric aerosol particle number concentrations that might be a significant source of cloud condensation nuclei  
357 and altering cloud albedo, structure and lifetime.

358 The experiments carried out in this work, designed to match atmospheric conditions as closely as possible, might  
359 be applicable to new particle formation and growth in the atmosphere, as ozone concentrations used in our study  
360 approached tropospheric levels, even at remote locations during spring and summer. SOA yields were calculated  
361 from the ratio of formed SOA amount to the amount of skatole reacted considering a density of the aerosol particles  
362 of  $1.0 \text{ g cm}^{-3}$ . The SOA yields varied significantly between the experiments with an average of 2.45%. In the  
363 literature, values for the SOA yield of skatole ozonolysis are not available. On the other hand, ozonolysis of  
364 biogenic terpenes have already been characterized in simulation chambers and values of SOA yields varied over a  
365 broad range: mass yields of 0.16 and 0.21 for  $\alpha$ -pinene ozonolysis were found<sup>59</sup> while some other studies reported  
366 SOA yields for the ozonolysis of monoterpenes between 0 and 76%<sup>60</sup>. Donahue et al.<sup>61</sup> explained the critical  
367 factors for SOA yield from terpene ozonolysis. The authors showed that different competing factors could affect  
368 the yield: the oxygenation that increases the absolute yield because the compounds are more polar and thus less  
369 volatiles; the potential difference between gas phase and condensed phase oxidation and oligomerization. The  
370 same authors suggested that SOA yields are likely to increase substantially through several generations of oxidative  
371 processing of the semi-volatile products. It has also been shown that the SOA yields are 80 to 100% larger for  
372 loadings above  $2 \mu\text{g m}^{-3}$ . Our low SOA yields compared to some of the monoterpenes might be explained by the  
373 aerosol mass loadings that were around  $3 \mu\text{g m}^{-3}$  but also by the presence of oxygenated compounds and the  
374 possible heterogeneous reactions at the sewage surface not taken into account in the yield calculations. Longer  
375 reaction time, from experiments conducted in larger facility would also lead to more oxidation, and thus increase  
376 the transfer from gas to particle phase. Our findings imply that during sewage sludge spreading, skatole is an  
377 important potential contributor to the formation of new particles under atmospherically relevant conditions. Since  
378 an increasing application of organic waste products is expected in continuously growing agricultural activities<sup>13</sup>,  
379 this additional VOC source may have a significant influence on atmospheric new particle formation and ozone  
380 reactivity during the spreading period. This study shows a novel mechanism involving indols from agricultural  
381 origin. Even though we cannot apply these values directly to the atmosphere, our results suggest that this skatole  
382 emission can change the chemistry and oxidative capacity of the atmosphere by its contribution to local



383 concentrations. Even if not realistic for atmospheric conditions, these processes can have a qualitative contribution  
384 to particle number as the high nucleation rate can induce locally and punctually a significant annual source of  
385 particle formation.

## 386 **Methods**

387 The experiments were performed in a poly(methyl methacrylate) chamber with Teflon walls (0.03 m<sup>3</sup>, 0.2 m  
388 height, 0.27 m width, 0.55 m length), built in a temperature-controlled room. A stainless steel container (0.52x  
389 0.27x0.02 m<sup>3</sup>) filled with the sewage sludge sample was used. High purity dry air (Air Liquide), passing through  
390 two Restek super clean gas filter kits for oxygen, moisture, and hydrocarbons removal (Restek, 22020) and an  
391 additional hydrocarbon trap (Restek 21991), was used for the experiments. Residence time of the air in the chamber  
392 was 5 min. Temperature and relative humidity in the chamber were 293 K and 40%, respectively. Before each  
393 experiment, the chamber was flushed with purified dry air for 30 min with a flow rate of 10 L min<sup>-1</sup> until the  
394 particle number concentration in the chamber was lower than 1 particle cm<sup>-3</sup>. When VOC concentrations reached  
395 an approximate steady state, ozone was injected reaching a chamber concentration of about 55 ppb. No OH or  
396 Criegee intermediates scavengers were added and no seed aerosol was used. Fifteen experiments with authentic  
397 sewage sludge samples (Supplementary Table S1) and two experiments with commercially available skatole  
398 (Sigma Aldrich >98.0% purity) were performed. Sewage sludge was sampled from the Colmar, France sewage  
399 treatment plant.

400 The gas and particle phases were continuously sampled. A high-resolution proton transfer reaction time-of-flight  
401 mass spectrometer <sup>36</sup> (HR-Qi-PTR-ToF-MS, Ionicon Analytik GmbH) was used to measure in real time the gas-  
402 phase VOC concentration (time resolution 1 s, m/z range 10–510). The drift tube pressure was set to 4 mbar, the  
403 temperature to 80 °C and the drift voltage to 1000 V, while the extraction voltage at the end of the tube (UD<sub>x</sub>) was  
404 44 V. The E/N was 132 Td (1 Td = 10<sup>-17</sup> V cm<sup>2</sup>). Protonated water (H<sub>3</sub><sup>18</sup>O<sup>+</sup>, m/z 21.022) protonated acetone  
405 (C<sub>3</sub>H<sub>7</sub>O<sup>+</sup>, m/z 59.049) and protonated diiodobenzene (PerMaSCal Ionicon, C<sub>6</sub>H<sub>5</sub>I<sub>2</sub><sup>+</sup>) ions and fragments (C<sub>6</sub>H<sub>4</sub>I<sub>2</sub>H<sup>+</sup>,  
406 m/z 330.941 and C<sub>6</sub>H<sub>5</sub>I<sup>+</sup>, m/z(203.943 respectively) were used for mass calibration. All data obtained by the PTR-  
407 ToF-MS were analyzed with the PTR-MS Viewer software (version 3.1.1, IONICON Analytik). O<sub>3</sub> was introduced  
408 into the chamber via an ozone generator (OSG-1, UVP) using purified dry air as carrier gas. The ozone at the  
409 entrance and at the exit of the chamber (41M, Environment SA), NO<sub>x</sub> (model 42i-TL, Thermo Fisher Scientific,  
410 Inc.), SO<sub>2</sub> (model 43C, Thermo Environmental Instruments), NH<sub>3</sub> (Picarro G2103), CO<sub>2</sub> and H<sub>2</sub>O (LICOR LI-  
411 840A) were continuously measured. VOCs were also trapped on Tenax TA cartridges for Thermal Desorption –  
412 Gas Chromatography – Mass Spectrometry (TD-GC-MS) analysis. The gas phase was sampled during 1 to 2 hours  
413 at 0.4 L min<sup>-1</sup>, and regulated with a mass flow controller (Bronkhorst). Tubes were desorbed using a thermo-  
414 desorption unit (TDU, Gerstel). VOCs separation was carried out using an Agilent 7890B gas chromatograph on  
415 a capillary column (30 m length, 0.25 mm inner diameter, 0.25 μm film thickness, HP-5MS Ultra Inert, Agilent).  
416 VOCs detection was performed with an Agilent 5977A mass selective detector. Ozone, NO<sub>x</sub> and SO<sub>2</sub> analysers  
417 have been calibrated before the experiments by the French air quality survey network. The PTR-ToF-MS has been  
418 calibrated using a Toluene standard of 102±10 ppb gas bottle diluted in zero air.

419 Particle number concentration and size distribution were measured using a scanning mobility particle sizer (SMPS  
420 3938; TSI) consisting of a differential mobility analyzer (DMA; TSI 3085) and a condensation particle counter  
421 (CPC; TSI 3788), extensively described elsewhere<sup>62</sup>. Sample flow was fixed at 0.6 L min<sup>-1</sup> and sheath flow at 6 L

422 min<sup>-1</sup>, providing measurements of the particle number and size distribution between 2.64 and 64 nm electrical  
423 mobility diameter. In the present study it was assumed that the wall loss rate was constant during experiments. All  
424 the values are wall and tube loss corrected (a maximum of 5% wall loss correction was applied to lower diameters)  
425 based on Kulkarni *et al.* (2011)<sup>63</sup>. Particle number and size distribution measured with the SMPS has been used  
426 to estimate the nucleation rates following the methodology described by Kulmala *et al.*<sup>64</sup>. The freshly formed  
427 secondary aerosols were collected during 3 – 5 hours on quartz fiber filters (Pall Tissuquartz QAT-UP 2500, 14  
428 mm diameter) in order to be chemically characterized by mass spectrometry techniques and liquid  
429 chromatography. The pristine sewage sludge surface chemical composition before ozonolysis was also analyzed  
430 by time-of-flight secondary ion mass spectrometry (TOF-SIMS). The TOF-SIMS analyses of bulk sewage sludge  
431 and filter-sampled particles were performed with an IONTOF TOF.SIMS<sub>5</sub> instrument equipped with a Bi<sub>3</sub><sup>+</sup> primary  
432 ion source. The energy of the Bi<sub>3</sub><sup>+</sup> ions was set to 25 keV and the used dose was ~ 2 10<sup>11</sup> ions cm<sup>-2</sup>, which matches  
433 the static mode in which only moderate fragmentation is expected<sup>65</sup>. Both positive and negative ion polarities  
434 were investigated with mass resolution  $m/\Delta m$  of 2000 and 3000, respectively.

435 Two-step laser mass spectrometry (L2MS) measurements were done using a Fasmatech S&T instrument already  
436 described elsewhere<sup>66</sup> with an average mass resolution of  $m/\Delta m \sim 8000$ . Desorption and ionization were achieved  
437 using two nanosecond Nd:YAG (Quantel Brilliant) pulsed lasers operated at 532 nm and 266 nm wavelength,  
438 respectively. Laser energies were adjusted to maximize the ion signal while limiting fragmentation of the parent  
439 species. Limit of detection as low as ~ 0.2 femtomole per laser pulse has been demonstrated in this configuration<sup>67</sup>.  
440 For UHPLC-HRMS analyses, the filters were extracted in methanol. 2 methyl indole, 5 methyl indole and 3 methyl  
441 indole (skatole) from Sigma Aldrich with >98.0% purity were used as analytical standards for UHPLC calibration.  
442 The UHPLC analyses were performed using an Acquity BEH C18 column (100x2.1mm, 1.7µm particle size,  
443 Waters). The mobile phase consisted in LC/MS grade acetonitrile/H<sub>2</sub>O/0.1% formic acid circulating at 0.3 mL  
444 min<sup>-1</sup> flowrate (gradient elution). The column temperature was set to 30°C and 10 µL of sample were used for  
445 injection. High-resolution mass spectrometry analysis was carried out with a Q-Exactive Orbitrap mass  
446 spectrometer (Thermo Fisher Scientific) in positive mode with a Heated ElectroSpray Ionization (HESI) probe  
447 using a high resolution full scan. The mass resolution was 70,000 in the full range  $m/z$  70 - 500.

#### 448 449 **Acknowledgements**

450 This work was supported by the French national programme LEFE/INSU (ENGRAIS) no 1762C0001, INRA EA  
451 department programme “Pari Scientifique” and ADEME (RAVISA) n° 1662C0006. This work also benefited from  
452 the support of the ANAEE-FR services 592 (ANR project n°11-INBS-0001). This work was also supported by the  
453 French National Research Agency (ANR) under contract ANR-18-CE22-0019 (UNREAL) and through the PIA  
454 (Programme d'Investissement d'Avenir) under contract ANR-10-LABX-005 (LABEX CaPPA – Chemical and  
455 Physical Properties of the Atmosphere).

456 The authors thank Brigitte Pollet and Pascale Lieben for UHPLC analysis and Denis Montenach and Magali Imhoff  
457 for the sewage sludge samples.

458

#### 459 **Author contribution**

460 R.C. designed the study, performed chamber experiments and wrote the manuscript. J.K., C. B., F.La., D.P.  
461 performed chamber experiments and/or analyzed the PTR-ToF-MS and SMPS data. C. D. performed GC-MS

462 analysis and analyzed the data. M. V., K. H., Y. C., C. F. performed the L2MS and SIMS experiments and analyzed  
463 the resulting data. M. B-D. helped with the UHPLC-HRMS mass spectrometer data. F.Le. and S.H. provided  
464 expertise in organic waste recycling and contributed to the manuscript. B.L., D.P. and I.K.O. contributed to the  
465 manuscript. C.F. did data interpretation, critical editing and review of the manuscript. All authors commented on  
466 the manuscript.

467

## 468 **References**

- 469 1. Burnett, R. *et al.* Global estimates of mortality associated with long-term exposure to outdoor fine  
470 particulate matter. *Proc. Natl. Acad. Sci.* **115**, 9592–9597 (2018).
- 471 2. Kroll, J. H. & Seinfeld, J. H. Chemistry of secondary organic aerosol: Formation and evolution of  
472 low-volatility organics in the atmosphere. *Atmos. Environ.* **42**, 3593–3624 (2008).
- 473 3. Lee, S.-H. *et al.* New Particle Formation in the Atmosphere: From Molecular Clusters to Global  
474 Climate. *J. Geophys. Res. Atmospheres* **124**, 7098–7146 (2019).
- 475 4. Kulmala, M. *et al.* Direct Observations of Atmospheric Aerosol Nucleation. *Science* **339**, 943–946  
476 (2013).
- 477 5. Kirkby, J. *et al.* Role of sulphuric acid, ammonia and galactic cosmic rays in atmospheric aerosol  
478 nucleation. *Nature* **476**, 429–433 (2011).
- 479 6. Almeida, J. *et al.* Molecular understanding of sulphuric acid–amine particle nucleation in the  
480 atmosphere. *Nature* **502**, 359–363 (2013).
- 481 7. Riccobono, F. *et al.* Oxidation Products of Biogenic Emissions Contribute to Nucleation of  
482 Atmospheric Particles. *Science* **344**, 717–721 (2014).
- 483 8. Kirkby, J. *et al.* Ion-induced nucleation of pure biogenic particles. *Nature* **533**, 521–526 (2016).
- 484 9. Ehn, M. *et al.* A large source of low-volatility secondary organic aerosol. *Nature* **506**, 476–479  
485 (2014).
- 486 10. Öström, E. *et al.* Modeling the role of highly oxidized multifunctional organic molecules for the  
487 growth of new particles over the boreal forest region. *Atmospheric Chem. Phys.* **17**, 8887–8901  
488 (2017).
- 489 11. Chrit, M. *et al.* Modelling organic aerosol concentrations and properties during ChArMEx summer  
490 campaigns of 2012 and 2013 in the western Mediterranean region. *Atmospheric Chem. Phys.* **17**,  
491 12509–12531 (2017).
- 492 12. Kulmala, M. *et al.* Formation and growth rates of ultrafine atmospheric particles: a review of  
493 observations. *J. Aerosol Sci.* **35**, 143–176 (2004).
- 494 13. Aneja, V. P., Schlesinger, W. H. & Erisman, J. W. Effects of Agriculture upon the Air Quality and  
495 Climate: Research, Policy, and Regulations. *Environ. Sci. Technol.* **43**, 4234–4240 (2009).

- 496 14. Lelieveld, J., Evans, J. S., Fnais, M., Giannadaki, D. & Pozzer, A. The contribution of outdoor air  
497 pollution sources to premature mortality on a global scale. *Nature* **525**, 367–371 (2015).
- 498 15. Vuolo, R. M. *et al.* Nitrogen oxides and ozone fluxes from an oilseed-rape management cycle: the  
499 influence of cattle slurry application. *Biogeosciences* **14**, 2225–2244 (2017).
- 500 16. Faburé, J. *et al.* Bibliography review of the agricultural contribution in atmospheric particles  
501 emissions: Identification of emission factors. *INRA Paris*, 164 pp. (2011).
- 502 17. Bauer, S. E., Tsigaridis, K. & Miller, R. Significant atmospheric aerosol pollution caused by world  
503 food cultivation. *Geophys. Res. Lett.* **43**, 5394–5400 (2016).
- 504 18. European Commission. Communication from the Commission to the Council and the European  
505 Parliament on future steps in bio-waste management in the European Union. [https://eur-  
506 lex.europa.eu/legal-content/EN/TXT/?uri=celex:52010DC0235](https://eur-lex.europa.eu/legal-content/EN/TXT/?uri=celex:52010DC0235) (2010).
- 507 19. Peltre, C. *et al.* RothC simulation of carbon accumulation in soil after repeated application  
508 of widely different organic amendments. *Soil Biol. Biochem.* **52**, 49–60 (2012).
- 509 20. Diacono, M. & Montemurro, F. Long-term effects of organic amendments on soil fertility. A review.  
510 *Agron. Sustain. Dev.* **30**, 401–422 (2010).
- 511 21. Gutser, R., Ebertseder, Th., Weber, A., Schraml, M. & Schmidhalter, U. Short-term and residual  
512 availability of nitrogen after long-term application of organic fertilizers on arable land. *J. Plant  
513 Nutr. Soil Sci.* **168**, 439–446 (2005).
- 514 22. Houot, S. *et al.* Agronomic Value and Environmental Impacts of Urban Composts Used in  
515 Agriculture. in *Microbiology of Composting* (eds. Insam, U. D. D. H., Sc, N. R. M. & Klammer, M. S.)  
516 457–472 (Springer Berlin Heidelberg, 2002). doi:10.1007/978-3-662-08724-4\_38.
- 517 23. Bianchini, A., Bonfiglioli, L., Pellegrini, M. & Sacconi, C. Sewage sludge management in Europe: a  
518 critical analysis of data quality. *Int. J. Environ. Waste Manag.* **18**, 226 (2016).
- 519 24. Kelessidis, A. & Stasinakis, A. S. Comparative study of the methods used for treatment and final  
520 disposal of sewage sludge in European countries. *Waste Manag.* **32**, 1186–1195 (2012).
- 521 25. Kumar, A. *et al.* Volatile organic compound emissions from green waste composting:  
522 Characterization and ozone formation. *Atmos. Environ.* **45**, 1841–1848 (2011).
- 523 26. Potard, K. *et al.* Organic amendment practices as possible drivers of biogenic Volatile Organic  
524 Compounds emitted by soils in agrosystems. *Agric. Ecosyst. Environ.* **250**, 25–36 (2017).
- 525 27. Liu, D., Nyord, T., Rong, L. & Feilberg, A. Real-time quantification of emissions of volatile organic  
526 compounds from land spreading of pig slurry measured by PTR-MS and wind tunnels. *Sci. Total  
527 Environ.* **639**, 1079–1087 (2018).
- 528 28. Feilberg, A., Bildsoe, P. & Nyord, T. Application of PTR-MS for Measuring Odorant Emissions from  
529 Soil Application of Manure Slurry. *Sensors* **15**, 1148–1167 (2015).

- 530 29. Nie, E. *et al.* Emission characteristics of VOCs and potential ozone formation from a full-scale  
531 sewage sludge composting plant. *Sci. Total Environ.* **659**, 664–672 (2019).
- 532 30. Rincón, C. A. *et al.* Chemical and odor characterization of gas emissions released during  
533 composting of solid wastes and digestates. *J. Environ. Manage.* **233**, 39–53 (2019).
- 534 31. Harrison, E. Z., Oakes, S. R., Hysell, M. & Hay, A. Organic chemicals in sewage sludges. *Sci. Total*  
535 *Environ.* **367**, 481–497 (2006).
- 536 32. Ni, J.-Q., Robarge, W. P., Xiao, C. & Heber, A. J. Volatile organic compounds at swine facilities: a  
537 critical review. *Chemosphere* **89**, 769–788 (2012).
- 538 33. Feilberg, A., Hansen, M. J., Liu, D. & Nyord, T. Contribution of livestock H<sub>2</sub>S to total sulfur emissions  
539 in a region with intensive animal production. *Nat. Commun.* **8**, (2017).
- 540 34. Byliński, H., Barczak, R. J., Gębicki, J. & Namieśnik, J. Monitoring of odors emitted from stabilized  
541 dewatered sludge subjected to aging using proton transfer reaction-mass spectrometry. *Environ.*  
542 *Sci. Pollut. Res. Int.* (2019).
- 543 35. Sánchez-Monedero, M. A., Fernández-Hernández, A., Higashikawa, F. S. & Cayuela, M. L.  
544 Relationships between emitted volatile organic compounds and their concentration in the pile  
545 during municipal solid waste composting. *Waste Manag.* **79**, 179–187 (2018).
- 546 36. Abis, L. *et al.* Profiles of volatile organic compound emissions from soils amended with organic  
547 waste products. *Sci. Total Environ.* **636**, 1333–1343 (2018).
- 548 37. Gebicki, J., Byliński, H. & Namieśnik, J. Measurement techniques for assessing the olfactory impact  
549 of municipal sewage treatment plants. *Environ. Monit. Assess.* **188**, 32 (2015).
- 550 38. Woodbury, B. L. *et al.* Emission of Volatile Organic Compounds after Land Application of Cattle  
551 Manure. *J. Environ. Qual.* **43**, 1207 (2014).
- 552 39. Sundberg, R. J. *The chemistry of indoles*. (Academic Press, 1970).
- 553 40. Wu, J. J. & Masten, S. J. Oxidation kinetics of phenolic and indolic compounds by ozone:  
554 applications to synthetic and real swine manure slurry. *Water Res.* **36**, 1513–1526 (2002).
- 555 41. Atkinson, R., Tuazon, E. C., Arey, J. & Aschmann, S. M. Atmospheric and indoor chemistry of gas-  
556 phase indole, quinoline, and isoquinoline. *Atmos. Environ.* **29**, 3423–3432 (1995).
- 557 42. Duncianu, M. *et al.* Development of a New Flow Reactor for Kinetic Studies. Application to the  
558 Ozonolysis of a Series of Alkenes. *J. Phys. Chem. A* **116**, 6169–6179 (2012).
- 559 43. Donahue, N. M., Drozd, G. T., Epstein, S. A., Presto, A. A. & Kroll, J. H. Adventures in ozoneland:  
560 down the rabbit-hole. *Phys. Chem. Chem. Phys.* **13**, 10848 (2011).
- 561 44. Khan, M. a. H., Percival, C. J., Caravan, R. L., Taatjes, C. A. & Shallcross, D. E. Criegee intermediates  
562 and their impacts on the troposphere. *Environ. Sci. Process. Impacts* **20**, 437–453 (2018).
- 563 45. Boy, M. *et al.* Oxidation of SO<sub>2</sub> by stabilized Criegee intermediate (sCl) radicals as a crucial source  
564 for atmospheric sulfuric acid concentrations. *Atmospheric Chem. Phys.* **13**, 3865–3879 (2013).

- 565 46. Chuong, B., Zhang, J. & Donahue, N. M. Cycloalkene Ozonolysis: Collisionally Mediated Mechanistic  
566 Branching. *J. Am. Chem. Soc.* **126**, 12363–12373 (2004).
- 567 47. Kroll, J. H., Sahay, S. R., Anderson, J. G., Demerjian, K. L. & Donahue, N. M. Mechanism of HOx  
568 Formation in the Gas-Phase Ozone-Alkene Reaction. 2. Prompt versus Thermal Dissociation of  
569 Carbonyl Oxides to Form OH. *J. Phys. Chem. A* **105**, 4446–4457 (2001).
- 570 48. Kurtén, T. & Donahue, N. M. MRCISD Studies of the Dissociation of Vinylhydroperoxide,  
571 CH<sub>2</sub>CHOOH: There Is a Saddle Point. *J. Phys. Chem. A* **116**, 6823–6830 (2012).
- 572 49. Mauldin III, R. L. *et al.* A new atmospherically relevant oxidant of sulphur dioxide. *Nature* **488**, 193–  
573 196 (2012).
- 574 50. Vereecken, L., Harder, H. & Novelli, A. The reaction of Criegee intermediates with NO, RO<sub>2</sub>, and  
575 SO<sub>2</sub>, and their fate in the atmosphere. *Phys. Chem. Chem. Phys.* **14**, 14682 (2012).
- 576 51. Ye, J., Abbatt, J. P. D. & Chan, A. W. H. Novel pathway of SO<sub>2</sub> oxidation in the atmosphere:  
577 reactions with monoterpene ozonolysis intermediates and secondary organic aerosol.  
578 *Atmospheric Chem. Phys.* **18**, 5549–5565 (2018).
- 579 52. Higgins, M. J. *et al.* Cycling of Volatile Organic Sulfur Compounds in Anaerobically Digested  
580 Biosolids and its Implications for Odors. *Water Environ. Res.* **78**, 243–252 (2006).
- 581 53. Zhu, Y. *et al.* Odor composition analysis and odor indicator selection during sewage sludge  
582 composting. *J. Air Waste Manag. Assoc.* **66**, 930–940 (2016).
- 583 54. Atkinson, R. *et al.* Evaluated kinetic and photochemical data for atmospheric chemistry: Volume I  
584 - gas phase reactions of Ox, HOx, NOx and SOx species. *Atmospheric Chem. Phys.* **4**, 1461–1738  
585 (2004).
- 586 55. Kurtén, T., Loukonen, V., Vehkamäki, H. & Kulmala, M. Amines are likely to enhance neutral and  
587 ion-induced sulfuric acid-water nucleation in the atmosphere more effectively than ammonia.  
588 *Atmospheric Chem. Phys.* **8**, 4095–4103 (2008).
- 589 56. Elm, J., Fard, M., Bilde, M. & Mikkelsen, K. V. Interaction of Glycine with Common Atmospheric  
590 Nucleation Precursors. *J. Phys. Chem. A* **117**, 12990–12997 (2013).
- 591 57. Parker, D. B. *et al.* Odorous VOC emission following land application of swine manure slurry.  
592 *Atmos. Environ.* **66**, 91–100 (2013).
- 593 58. Joutsensaari, J. *et al.* Nanoparticle formation by ozonolysis of inducible plant volatiles.  
594 *Atmospheric Chem. Phys.* **5**, 1489–1495 (2005).
- 595 59. Xavier, C. *et al.* Aerosol mass yields of selected biogenic volatile organic compounds - a theoretical  
596 study with nearly explicit gas-phase chemistry. *Atmospheric Chem. Phys.* **19**, 13741–13758 (2019).
- 597 60. Lee, A. *et al.* Gas-phase products and secondary aerosol yields from the ozonolysis of ten different  
598 terpenes. *J. Geophys. Res.* **111**, D07302 (2006).

- 599 61. Donahue, N. M. *et al.* Critical factors determining the variation in SOA yields from terpene  
600 ozonolysis: A combined experimental and computational study. *Faraday Discuss.* **130**, 295 (2005).
- 601 62. Kammer, J. *et al.* Observation of nighttime new particle formation over the French Landes forest.  
602 *Sci. Total Environ.* **621**, 1084–1092 (2018).
- 603 63. Kulkarni, P., Baron, P. A. & Willeke, K. *Aerosol Measurement: Principles, Techniques, and*  
604 *Applications.* (John Wiley & Sons, Inc., 2011).
- 605 64. Kulmala, M. *et al.* Measurement of the nucleation of atmospheric aerosol particles. *Nat. Protoc.*  
606 **7**, 1651–1667 (2012).
- 607 65. Irimiea, C. *et al.* A comprehensive protocol for chemical analysis of flame combustion emissions  
608 by secondary ion mass spectrometry. *Rapid Commun. Mass Spectrom.* **32**, 1015–1025 (2018).
- 609 66. Duca, D. *et al.* On the benefits of using multivariate analysis in mass spectrometric studies of  
610 combustion-generated aerosols. *Faraday Discuss.* **218**, 115–137 (2019).
- 611 67. Faccinetto, A., Focsa, C., Desgroux, P. & Ziskind, M. Progress toward the Quantitative Analysis of  
612 PAHs Adsorbed on Soot by Laser Desorption/Laser Ionization/Time-of-Flight Mass Spectrometry.  
613 *Environ. Sci. Technol.* **49**, 10510–10520 (2015).
- 614